Computational analysis of transport across flake-filled composites of realistic microstructure

Cite as: AIP Conference Proceedings **2065**, 030039 (2019); https://doi.org/10.1063/1.5088297
Published Online: 06 February 2019

Andreas Tsiantis, Sholpan Sumbekova, and Thanasis D. Papathanasiou

Computational Analysis of Transport Across Flake-Filled Composites of Realistic Microstructure

Andreas Tsiantis[1)], Sholpan Sumbekova[2)] and Thanasis D. Papathanasiou.[1,2,a)]

[1]*University of Thessaly, Department of Mechanical Engineering, Volos, Greece*
[2]*Nazarbayev University, Department of Chemical Engineering, Astana, Kazakhstan*
[a)]Corresponding author: athanasios.papathanasiou@nu.edu.kz

Abstract. In this paper we present the results of a computational study of diffusion across disordered flake composites in which the flakes are misaligned with respect to the direction of bulk diffusion. We evaluate the effect of flake orientation as well as the influence of boundary conditions and unit-cell types on the predicted barrier properties. Flake orientation impacts very significantly on the barrier properties in flake-filled composites, and usually the key objective in their fabrication is to orient them as close as possible to being perpendicular to the direction of macroscopic diffusion. Our computations are carried out in two-dimensional, doubly-periodic unit cells, each containing up to 3000 individual flake cross-sections. We consider high aspect ratio (α) systems with α=1000, from the dilute ($\alpha\varphi$=0.01) and into the very concentrated ($\alpha\varphi$=40) regime. The effective diffusivity of the corresponding unit cells is computed from the imposed concentration difference and the computed mass flux, using Fick's Law. We show that use of cyclic boundary conditions and doubly-periodic unit cells results in effective diffusivities which are in agreement with theory and invariant of the shape of the unit cell. We also show that the use of adiabatic boundary conditions produces erroneous results at high flake concentrations. Finally we compare our results to the predictions of existing literature models and find that the latter deviate significantly from computation at high flake concentrations.

Keywords: Flake composites; barrier properties; microstructure; misorientation
PACS: 82.35.Lr; 68.60.-p, 66.30.Pa, 65.80.Ck

INTRODUCTION

Flake-filled composites are often used as barrier materials, among others in food packaging, since their presence hinders the diffusion of gasses (O_2, CO_2, H_2O) to and from a container, by increasing the tortuosity of the medium. At the same time, the advantages of formability and design characterizing plastic materials are maintained. Flakes of inorganic materials (mica), nano-scale mineral platelets such as montmorillonite as well as graphene-oxide platelets of aspect ratios well over 1000, have been used for this purpose [1,2]. It is known that incorporation of such fillers aligned perpendicular to the direction of macroscopic diffusion is very effective in increasing the barrier properties. Both theoretical results and computational studies have shown that, for flakes aligned perpendicular to the direction of macroscopic diffusion, the improvement in the Barrier Improvement Factor (BIF) ranges from being $\sim(\alpha\varphi)$ in dilute systems, where (α) is the aspect ratio and (φ) the volume fraction of the flakes, to being $\sim(\alpha\varphi)^2$ in more concentrated dispersions [3-7]. When the orientation of the flakes deviates from perfect alignment, it is known that the BIF decreases; however no universally accepted models to predict this effect exist and only limited computational results have been presented, with the exception of the recent studies of [7-9]. This is unfortunate, since the topic of flake misalignment and its effect on BIF is definitely of practical interest;manufactured flake composites produced via melt processing are never characterized by perfect flake alignment. There have been several models proposed in order to describe the effect flake misalignment. These can be broadly categorized as based on (i) the ad-hoc incorporation of orientation metrics in existing models [2,9,10] or (ii) the derivation of the effective diffusion coefficient from diffusion path calculations [11-13]. In this study we compare their predictions to computational results and also address the issue of boundary conditions and RVE types in computation.

Proceedings of PPS-34
AIP Conf. Proc. 2065, 030039-1–030039-4; https://doi.org/10.1063/1.5088297
Published by AIP Publishing. 978-0-7354-1793-9/$30.00

RESULTS AND DISCUSSION

We generate the geometries on which computations are carried out using a Random Sequential Algorithm (RSA). The RSA places up to 3000 individual cross-sections inside an initial rectangular geometry. The planar coordinates of the center of each flake are defined using a random number generator, whereas the orientation angle (θ) is the same and fixed for all flakes. At each flake placement attempt, the algorithm conducts checks for overlap of the last-placed flake with existing ones in a sub-region surrounding the center of the last-placed flake (this feature impacts on scalability and speed of the algorithm), and, if no overlap is detected, continues with the placement of the next flake, until the desired number of flakes has been placed, or, until no flake can be placed after 10^5 attempts. Further details have been presented in [7,8]. A minimum allowable distance (2t) between flakes is imposed, where (t) is the thickness of the flake; this is necessary so that the resulting geometry can be subsequently meshed. If the dimensions of the unit cell are (H) and (L) and if it contains (N) flakes of dimensions (t, α), the flake area fraction (φ) is $\varphi = N\alpha t^2/LH$ and the length (l) of each flake is $l = \sqrt{LH(\alpha\phi)/\mathrm{N}}$.

Cyclic boundary conditions are used on the right and left boundaries, specifically $C_{left}(0,y)=C_{right}(L,y)$, where (C) is the solute concentration. The concentration (C) is fixed on the top and bottom boundaries, so that a macroscopic concentration difference (ΔC) is established. Since the flakes are impermeable, it is $\partial C/\partial \mathbf{n} = 0$ on their surfaces. At each pair of (α) and (φ) we generate ~10 different geometries; these differ in flake placement but are characterized by the same flake orientation. The mesh generating program GMSH is used to generate the computational meshes, each containing ~4x10^6 triangular elements. These meshes are subsequently used by the open source packageOpenFoam to solve the steady-state diffusion equation $\nabla^2 C = 0$ and provide the distribution of the solute concentration (C) as well as the value of ($\partial C/\partial \mathbf{n}$) at every point in thegeometry of interest. As a result, the mass flux across any line in the domain, including the top (or bottom) boundary, on which (C) is constant, can be calculated using $J_n = -D_0 \int_0^L (\frac{\partial C}{\partial \mathbf{n}}) dx$, where **n** is the outward unit vector and (L) is the width of the unit cell.

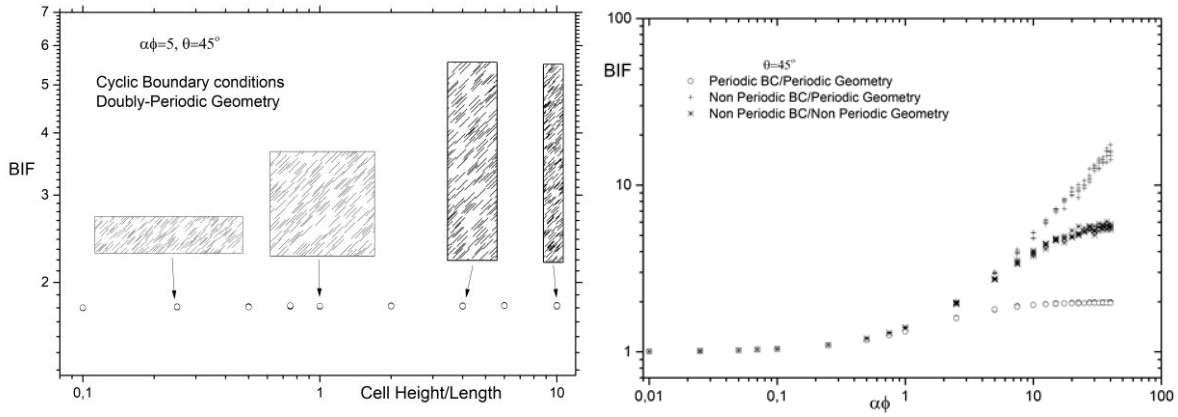

FIGURE 1: (Left) Computational results showing the predicted Barrier Improvement Factor (BIF ~$1/D_{eff}$) as function of the aspect ratio (H/L) of the unit cell. (Right) Effect of type of boundary conditions and geometry used on teh BIF, for all flake concentrations (αφ) studied.

If D_{eff} is the effective diffusivity of an equivalent representative material, equating this flux with the one obtained from Fick's law we obtain $D_{eff} = \frac{HD_0}{\Delta C \cdot L} \int_0^L (\frac{\partial C}{\partial \mathbf{n}}) dx$. In Figure (1) we show that the type of geometry and the type of boundary conditions have an influence on D_{eff}.We have carried out extensive comparisons of the BIFs predicted through the use of unit cells having (i) doubly-periodic geometry, (ii) geometry in which flakes were excluded from crossing boundaries, (iii) cyclic boundary conditions and (iv) adiabatic boundary conditions. Characteristics (iii) and

(iv) refer to the boundary condition applied on the two vertical sides of the unit cell (the two horizontal sides being at constant concentration). Such a comparison is shown in Figure (1), which shows computational results for the predicted effective diffusivity (D_{eff}) for $\alpha\varphi=5$ and $\theta=\pi/4$ and various shapes of unit cells. Use of doubly periodic unit cells results in the elimination of the effect of the dimensions and aspect ratio of the computational domain on the computed effective diffusivity, and thus, renders the studied geometries true RVEs. Alternative approaches [7,9] result in artifacts, such as oriented or depleted layers adjacent to boundaries, and thus in predictions of D_{eff} which are not geometry-invariant. Figure (1) also shows predicted values of the BIF as function of ($\alpha\varphi$) for various combinations of unit cell type and boundary conditions.In earlier studies, Chen and Papathanasiou [7] and Dondero and co-workers [9] used non-periodic unit cells and adiabatic conditions on the side boundaries of the unit cells. Being aware that this would have some impact on the predicted diffusivities, both, as a result of flake layers forming adjacent to unit-cell walls as well as a result of artificially restricting diffusion across these boundaries, the effective diffusivity was computed from a central region of their unit cells. While correct, this is certainly inefficient and does not offer a clear estimate of possible errors or any guidance on the required size of this internal region.In this study we conclusively show that while the effect of unit cell type and/or boundary conditions is very small for dilute systems, thus validating earlier studies [6,8], major differences exist for $\alpha\varphi>5$ – this is incidentally the concentration beyond which no results have been reported in the literature this far. In this study we conclusively show that only the combination of periodic geometry with periodic boundary conditions will result in invariant results at all flake loadings.

For misaligned flake systems, taking into account the rotational properties of the diffusivity tensor, which dictates that $D_{eff}(\theta) = D_{11}\cos^2(\theta) + D_{22}\sin^2(\theta) = D_{11} + (D_{22} - D_{11})\sin^2(\theta)$ and by utilizing the models of Lape et al. [4] and Nielsen [14] for the principal diffusivities D_{11} and D_{22} respectively, Tsiantis and Papathanasiou [8] proposed the following model for D_{eff}.

$$\frac{D_{eff}(\theta)}{D_0} = \frac{(1-\phi)}{(1+\alpha\phi/\lambda)^2}\cos^2(\theta) + \frac{(1-\phi)}{1+\phi/2\alpha}\sin^2(\theta) \qquad (1)$$

This model was found to be in excellent agreement with computational predictions for $0<\theta<\pi/2$ and $\alpha\varphi\leq 40$. A key result of both, this model and of the computational results of [8] is the fact that at $\theta>0$ the BIF ($\sim 1/D_{eff}$) does not grow monotonically with ($\alpha\varphi$) but instead it reaches a plateau value; this plateau value decreases as (θ) increases, and as (θ) approaches zero the effective diffusivity approaches the (plateau) value implied by the Nielsen model [14]. In Figure (2) we present a comparison of the results of Eq.(1) as well as of computational results to various existing literature models [10-13]. It is clear that severe discrepancies are observed at large flake loadings and this warrants further study of the topic.

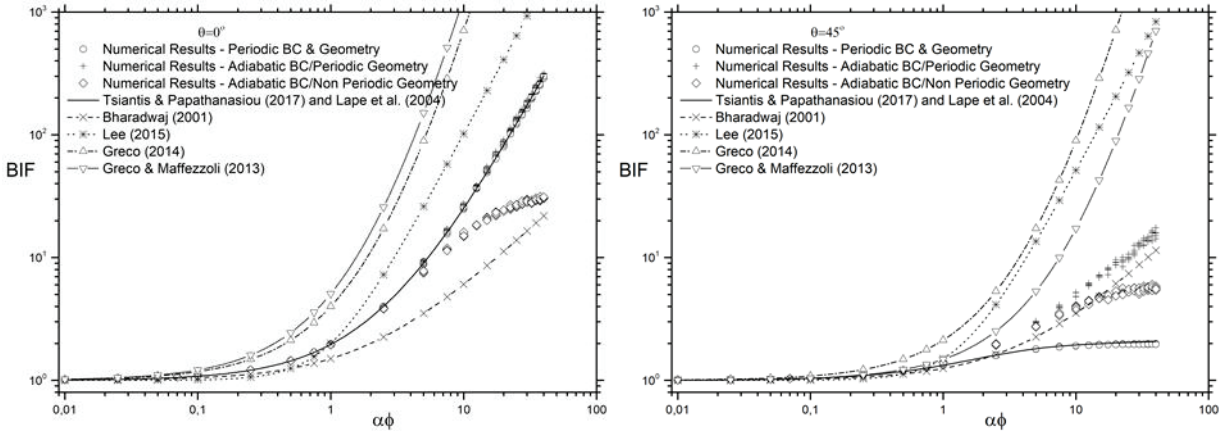

FIGURE 2. Predicted values of the BIF as function of flake concentration ($\alpha\varphi$) for various combinations of geometry (periodic/non-periodic) and boundary conditions on the side walls (cyclic/adiabatic). Two values of the misalignment angle and H/W=1.

Contour maps of concentration are shown in Figure (3), while Figure (4) shows an example three-dimensional geometry including randomly placed and randomly oriented flakes; we are currently working at evaluating the effect that the consideration of a 3D realistic microstructure has on the predicted BIF as well as how these predictions compare to theoretical models.

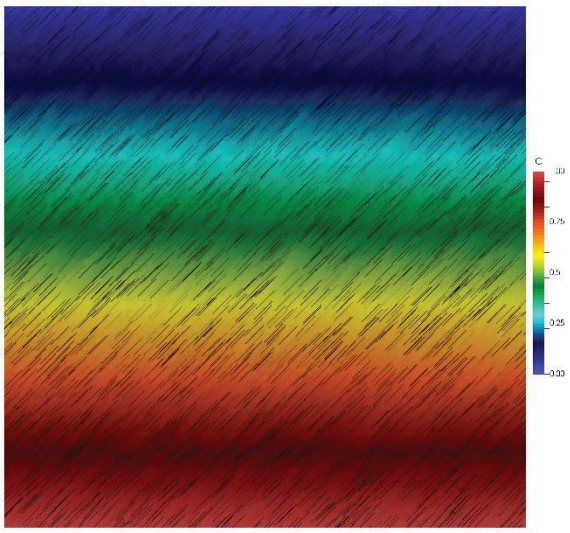

FIGURE 3. Concentration profiles in systems with αφ=10, θ=45o. The flakes are also visible. N=3000

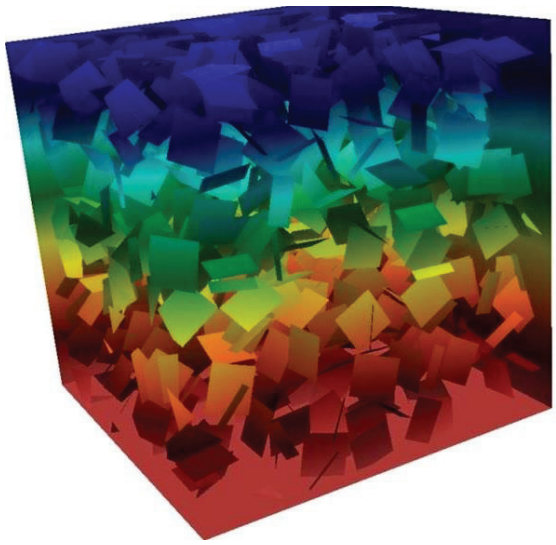

FIGURE 4. 3D geometry and the computed corresponding concentration profiles. Randomly placed and randomly oriented flakes.

CONCLUSION

We have presented the results of a computational evaluation of the effect of misalignment on the effective properties of composites filled with high aspect ratio flakes. We analyze the results and compare them to the predictions of existing theoretical models, including one which the barrier properties of the composite are related to the two principal diffusivity, and thus, to flake loading (αφ) as well as (θ). Predictions of existing models are in substantial variance to computational results at high flake loadings. We also examine the effect of boundary conditions on the predicted effective diffusivity. Our results show that at higher flake loading, use of adiabatic boundary conditions at the side walls of the unit cell will result in erroneous predictions for the effective diffusivity. We show that use of cyclic conditions will result in effective diffusivities which are, as expected, unaffected by the shape of the unit cell.

REFERENCES

1 Lagaron JM, Nunez E. Journal of Plastic Film and Sheeting 2011;28(1):79-89.
2 Lee K-H, Hong J, Kwak SJ, Park M, Son JG. Carbon 2015;83:40-47.
3 Cussler EL, Hughes SE, Ward WJ, Aris R. J. Membr. Sci. 1988; 38:161-74.
4 Lape NK, Nuxoll EE, Cussler EL. J. Membr. Sci. 2004;236:29–37.
5 Lebovka N, Khrapatiy S, Vygornitskyi,Pivovarova N. Physica A, 2014; 408:19-27.
6 Chen X, Papathanasiou T.D. Journal of Plastic Film and Sheeting, 2007;23:319-346.
7 Papathanasiou TD. Tsiantis A. Journal of Plastic Film and Sheeting, 2017, 33(4), 438-456
8 Tsiantis, A. and Papathanasiou, T.D. Materials Sciences and Applications , 2017, 8, 234-246
9 Dondero M. Tomba JP. Cisilino AP. J. Membr. Sci. 2016;514:95-104.
10 Bharadwaj RK. Macromolecules 2001;34:9189–9192.
11 Greco A. Computational Materials Science 2014;83:164-170.
12 Greco A, Maffezzoli A., J. Membrane Science. 2013; 442:238-244
13 Sorrentino A, Tortora M, Vittoria V. Journal of Polymer Science: Part B: Polymer Physics 2006;44:265-274.
14 Nielsen LE. Journal of Macromolecular Science Part A- Chemistry 1967;5(1):929-942.